Open Access

Recent Progress in Materials

LIDSEN Publishing Inc.

Original Research

Experimental and Analytical Studies of an Ultra-high Performance Concrete Beam Using Carbon Fiber Reinforced Polymer Bars

C. Shawn Sun [1, *], Nahid Farzana [2], Dinesha Kuruppuarachchi [3], Mohammadamin Azimi [4], Huayuan Zhong [5]

1. California State University, 18111 Nordhoff Street, Northridge, CA, USA; E-Mail: shawn.sun@csun.edu
2. Louisiana Tech University, 600 Dan Reneau Dr., Ruston, LA, USA; E-Mail: nfa004@latech.edu;
3. Crosby Group, 155 Bovet Road, Suite 550, San Mateo, CA, USA; E-Mail: dkuruppuarachchi@crosbygroup.com
4. GeoEngineers Inc., 13220 Evening Creek Drive South, Suite 115, San Diego, CA, USA; E-mail: aazimi@geoengineers.com
5. CSRS Inc., 8555 United Plaza Blvd, Baton Rouge, LA, USA; E-mail: hyzhong89@gmail.com

* **Correspondence:** C. Shawn Sun; E-Mail: shawn.sun@csun.edu

Academic Editor: Mostafa Seifan

Special Issue: New Trends on Construction Technologies and Sustainable Building Materials

Recent Progress in Materials
2023, volume 5, issue 2
doi:10.21926/rpm.2302019

Received: September 10, 2022
Accepted: April 05, 2023
Published: May 04, 2023

Abstract

Infrastructure degradation attributable to concrete deterioration and corrosion of reinforcing steel has been a long-standing challenge to the owners and engineers. This problem becomes more evident when concrete structures are subject to aggressively corrosive environments. The use of advanced materials such as ultra-high performance concrete (UHPC) and carbon fiber reinforced polymer (CFRP) bars has a strong potential to overcome this challenge and help build new infrastructure that is durable and sustainable. However, structural behavior of members using both UHPC and CFRP bars has not been studied thoroughly in the United States and overseas, and no codes or specifications are readily available for structural engineers to follow. This paper presented an initial attempt to explore this topic by addressing

the bond behavior between UHPC and CFRP bars through pullout tests. The test results showed that the UHPC specimens exhibited gradually increased slippage after the peak load and demonstrated superior bond performance in comparison with the conventional concrete specimens. Flexural tests were also conducted to compare the structural behavior of two large-scale beams, which were made of conventional concrete reinforced by steel bars and UHPC reinforced by CFRP bars, respectively. Test results showed that the UHPC beam did not exhibit as much ductility as the conventional beam, as predicted. However, there was still sufficient warning of impending failure in a form of extensive cracking and substantial deflection attributable to the bridging effect of the steel fibers. Further, flexural strength analysis of the UHPC beam using CFRP bars was discussed satisfying strain compatibility and force equilibrium, which provided a guidance for structural engineers to design such members. The research approach adopted in this paper may be applicable to study UHPC beams using other types of FRP materials.

Keywords
Ultra-high performance concrete; carbon fiber reinforced polymer bars; pullout; bond mechanism; flexural strength; strain compatibility; force equilibrium

1. Introduction

Infrastructure degradation attributable to concrete deterioration and corrosion of reinforcing steel is a major economic and societal issue in the U.S. that costs billions of dollars annually [1]. Concrete deteriorates for a variety of reasons, but corrosion of steel reinforcement has been one of the most prevalent mechanisms of deterioration since concrete structures were introduced in the early 1900s [2]. It affects many types of concrete elements, including marine structures, bridges, and other structures subjected to severe environments and weather. Ingress of chloride ions from the environment is the predominant cause of concrete structures' deterioration. Consequently, it degrades structures' durability and reduces their service life severely [3]. For example, steel reinforcement used in marine substructures has exhibited corrosion damage within twenty years of construction (Figure 1) [4].

Figure 1 Corrosion in precast prestressed concrete piles [4].

Numerous failures or deficiencies of reinforced and prestressed concrete structures have been reported because of steel corrosion in recent history. These failed or deficient structures include buildings, bridges, marine structures, waterways and ports, etc. Further, approximately 13% of the nation's 595,000 bridges have been classified as structurally deficient [5]. The projected average cost of maintaining these bridges is $8.3 billion annually, with a cost of upwards of $150 billion to improve the condition of existing infrastructure. A significant portion of these deficiencies are attributable to corrosion of steel reinforcement because of the use of de-icing salts and/or exposure to coastal environments [6].

The problem of concrete deterioration is particularly notable in structures subjected to aggressively corrosive environments and weather, including wastewater tanks and cooling towers in electrical plants. Field assessment of reinforced concrete cooling towers exposed to harsh operating environments has found severe corrosion of embedded steel reinforcement, concrete delamination and spalling [7]. The use of advanced materials such as ultra-high performance concrete (UHPC) and carbon fiber reinforced polymer (CFRP) bars has a strong potential to overcome this challenge and help build new infrastructure that is durable and sustainable. The following sections briefly describe the primary characteristics and current use of CFRP bars and UHPC in the United States.

1.1 Current Use of CFRP Bars

CFRP reinforcement is a composite, high-strength, elastic, brittle, and orthotropic material. The carbon fibers used commonly have exceptionally high tensile strength–to–weight ratios, with a strength ranging from 1,970 to 3,200 MPa [8]. These fibers also have a low coefficient of linear expansion and high fatigue strength. However, compared to steel reinforcement, the disadvantages of most CFRP reinforcement include weaker shear resistance, lower compressive strength, a lower modulus of elasticity, and a higher cost [9, 10]. Design specifications are available today in Canada, Japan, China, and Europe. In the U.S., the American Concrete Institute Committee 440 published guidelines for the design and construction of FRP-reinforced concrete structures [11]. A significant research project funded by the Transportation Research Board entitled, "Guide Specification for the Design of Concrete Bridge Beams Prestressed with CFRP Systems" was completed recently and its

research findings were incorporated into the AASHTO LRFD Bridge Design Specifications [12, 13]. Therefore, CFRP reinforcement is becoming a recognized alternative to traditional steel reinforcement with a wide range of applications.

1.2 Current Use of UHPC

Advances in concrete materials technology have led to the development of a new generation of cementitious materials referred to as UHPC, which has mechanical and durability properties that far exceed those of conventional concrete. Conventional concrete's compressive strength generally ranges from 27.5 to 55 MPa, while UHPC's compressive strength is greater than 124.1 MPa, 2 to 5 times higher than that of conventional concrete [14]. UHPC is a cementitious composite material composed of an optimized gradation of granular constituents, a water-to-cementitious materials ratio less than 0.25, and a high percentage of discontinuous internal fiber reinforcement. UHPC formulations often consist of a combination of Portland cement, fine sand, silica fume, high-range water-reducing admixture (HRWR), fibers (usually steel), and water. More importantly, UHPC's dense microstructure decreases its porosity and consequently, its permeability. Researchers have conducted extensive laboratory and field tests and confirmed UHPC's exceptionally high durability. Chloride penetration tests on UHPC specimens have indicated that corrosion of discontinuous steel fibers in the concrete mix occurs typically on and very close to the surface, and it does not progress into the interior of the UHPC specimens [15]. Thus, the use of UHPC can improve durability properties and increase the service life of structures.

UHPC has been used successfully in several countries, including Canada, the UK, Germany, Japan, South Korea, and Malaysia, and has been proven to improve structures' durability properties and increase their service life. Therefore, UHPC's use has the strong potential to overcome the long-lasting challenge of infrastructure deterioration. The Federal Highway Administration (FHWA) has led the efforts to promote UHPC's implementation in bridges. UHPC has been used successfully in buildings, bridges, marine structures, and underground facilities.

1.3 Bond Characteristics between UHPC and CFRP Rebar

The bond characteristics of reinforcement are of paramount importance in achieving a fundamental understanding of the structural behavior of concrete members. The introduction of UHPC is expected to enhance the bond behavior of reinforcement in concrete structures. Experimental studies have been conducted for steel bars embedded in UHPC. Tests on steel bars revealed that the bridging effect provided by the steel fibers in UHPC after cracking could provide effective post-cracking tensile capacity to the concrete matrix and limit crack widths, thereby resulting in improved bond resistance [16].

Numerous researchers have investigated the bond behavior of CFRP bars embedded in conventional concrete. The mode of CFRP bars' bond failure differs substantially from that of deformed steel bars because of damage to the resin-rich surface of the bars when pullout occurs [17]. The interlaminar shear strength just below the resin-rich surface layer of the bar affects a CFRP bar's bond strength. Several researchers have studied the effect of concrete compressive strength on CFRP bars' bond strength [18, 19] and found that an increase in concrete strength results in increased bond strength.

1.4 Need for a Combined Use of UHPC and CFRP Bars

A successful use of UHPC and CFRP bars in civil infrastructure, particularly structures subjected to severely corrosive environments and weather, can mitigate or eliminate concrete deterioration and corrosion of steel reinforcement, which has major economic and societal ramifications in the United States. Successful implementation of these advanced materials allows significant enhancement of long-term structural durability and sustainability, potential cost savings in future maintenance, repair, and rehabilitation, and substantial improvement in public safety. Possible examples of applications include coastal bridge substructures, marine structures, wastewater tanks, and cooling towers in electrical power plants.

Justifications of using members made of UHPC and CFRP in structures subjected to severely corrosive environments and weather are summarized below:

- CFRP reinforcement features noncorrosive characteristics, a high strength–to–weight ratio, and good fatigue properties [20]. Thus, its use can eliminate steel reinforcement corrosion completely.
- UHPC is recognized for its exceptional strength, ductility, and durability. Its dense matrix prevents deleterious solutions from penetrating into the matrix, which results in greater resistance to deterioration compared to conventional concrete.
- Using UHPC or CFRP reinforcement alone may not completely resolve the corrosion issues. Reasons include: 1) Due to the low water–binder ratio and highly exothermic hydration reaction, early-age cracking of UHPC has been reported during the manufacturing process [21, 22]. As a result, conventionally reinforced (or non-prestressed) UHPC members using steel reinforcement are subject to corrosion risk under corrosive environments; and 2) If UHPC is not included, the regular concrete can deteriorate and impair the bond between the concrete and CFRP reinforcement. Therefore, the use of CFRP reinforcement in UHPC members appears to be a necessary solution in fully eliminating the corrosion concerns.
- UHPC's exceptional properties can mitigate the disadvantages of CFRP reinforced concrete members because extensive cracking is expected prior to the sudden failure of the CFRP reinforcement, which provides additional warning and contributes to enhancing structural safety.
- Without resorting to prestressing, production of the UHPC members reinforced by CFRP bars eliminates the need for special pretensioning facilities and, therefore, simplifies and accelerates the production.

Currently, the costs of UHPC and CFRP bars are significantly higher than that of conventional concrete and steel reinforcement. However, the use of UHPC and CFRP reinforcement can be cost-competitive if the life-cycle cost of a structure is considered. The entire life cost of a structure encompasses future maintenance, repair, and rehabilitation costs, in addition to the initial cost [23]. For example, the Michigan Department of Transportation used CFRP bars and strands in all superstructure elements of the M-102 over Plum Creek Bridge recently. The use of CFRP reinforcement cost 23% more than did steel reinforcement. Nevertheless, this additional cost can be justified readily because the use of CFRP reinforcement offsets the future maintenance and repair costs appreciably.

The combined use of UHPC and CFRP in structural members has not been studied thoroughly in the U.S. and overseas [24-26]. This paper presents an initial attempt to study the structural behavior

of such members. It describes the bond behavior between UHPC and CFRP through pullout tests, and discusses the large-scale beam tests in the lab. Two types of beams were tested: 1) a beam made of conventional concrete and steel rebar that serves as a baseline for comparison purposes; and 2) a beam made of UHPC and CFRP rebar. In addition, the flexural strength analysis of beams consisting of UHPC and CFRP bars is discussed.

2. Materials and Methods

2.1 Bond Behavior between UHPC and CFRP Rebar

2.1.1 Material Properties of Pullout Specimens

The bond mechanisms of CFRP reinforcement differ from those of steel reinforcement because CFRP materials are anisotropic [27-29]. The interface bond mechanisms between CFRP bars and UHPC are attributable to chemical and friction bonds. Pullout tests were conducted to understand the interface bond mechanisms of CFRP bars embedded in UHPC by formulating the bond stress versus slip characteristics of CFRP reinforcement.

The mechanical properties of CFRP bars and UHPC affect the bond mechanisms. According to the CFRP supplier, sand-coated Aslan #10 bars had a tensile strength of 2,817.3 MPa and modulus of elasticity of 130.9 GPa. A commercial UHPC product, Ductal JS1000 premix with 2% steel fibers (by volume), was used. Figures 2a and 2b show the IMER 750 mixer and steel fibers, respectively. The steel fibers had a nominal diameter of 0.2 mm and a nominal length of 13 mm. Figure 2c depicts the UHPC during mixing. Figures 3a and 3b show a 76 mm × 152 mm cylinder before and after compression tests, respectively. Compression tests of the UHPC cylinders were performed using a modified version of ASTM C39/C39M [30]. Cylinders were untreated, stripped at 48 hours, and achieved a compressive strength of 130.9 MPa at 14 days when pullout tests were performed.

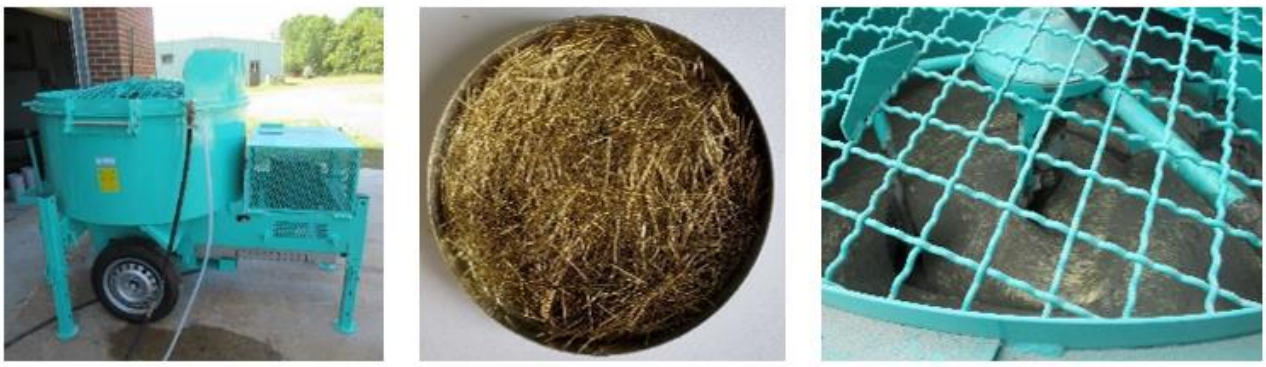

Figure 2 UHPC production. (a) IMER 750 mixer. (b) Steel fibers. (c) UHPC during mixing.

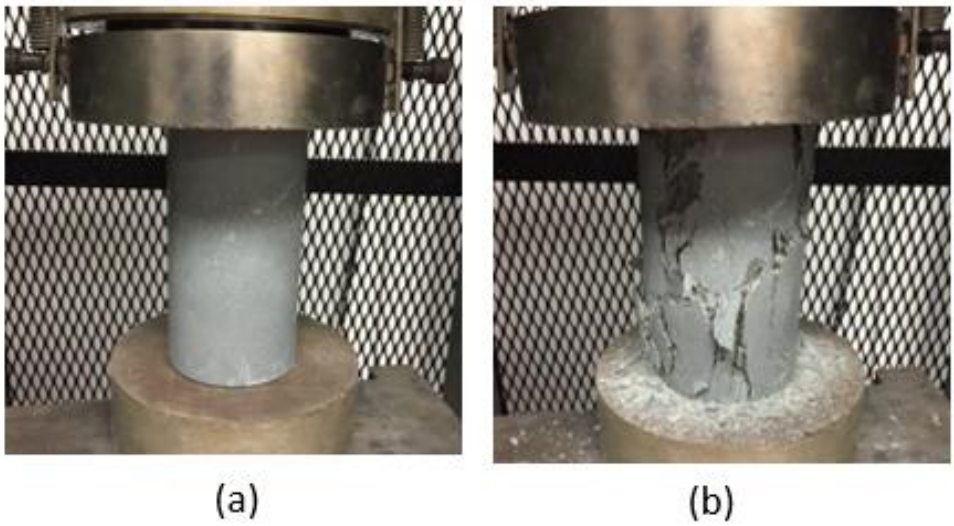

Figure 3 Compression tests of a UHPC cylinder. (a) 76 mm × 152 mm cylinder before testing. (b) cylinder after testing.

2.1.2 Pullout Test Setup

As shown in Figure 4a, a concrete block was held in position under a pair of channels that were anchored to a structural steel frame using two vertical threaded rods. An MTS machine was used to apply the load at a rate of 0.0254 mm per second. The pullout tests included four specimens made of UHPC blocks and CFRP bars (Figure 4b). Each specimen consisted of a #10 CFRP bar centrally embedded in a UHPC block with dimensions of 152 mm × 152 mm × 102 mm. The bar embedment length is 102 mm. Because the MTS machine grip was unable to hold the CFRP tightly, one end of the CFRP bar was housed in a steel pipe filled by high-strength grout. One pipe end was welded to a steel T-section connected with the grip using a bolt. For comparison purposes, four specimens made of conventional concrete and steel rebar (Grade 414 MPa, #13) were also tested. Figure 4c shows a photo of one specimen, in which the concrete had a compressive strength of 41.4 MPa.

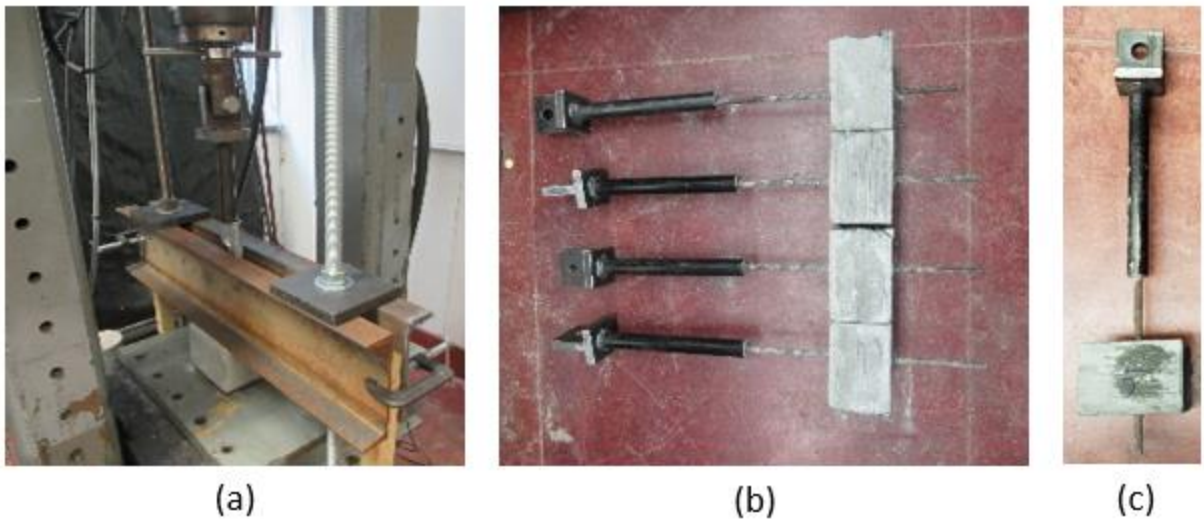

Figure 4 Pullout tests. (a) test setup. (b) specimens made of UHPC and CFRP bar. (c) specimen made of conventional concrete and steel bar.

2.2 Large-scale Testing of Beams

2.2.1 Descriptions of Large-scale Tests

Pullout tests are accepted widely to evaluate the bond behavior because of their simplicity and ability to isolate various parameters' effects on bond performance. Flexural tests of large-scale beams, however, are essential to supplement the pullout tests because beam tests represent the actual stress state in a concrete structure as closely as possible [31]. Further, flexural tests of large-scale beams are more reliable than pullout tests because they account for the global effect, including influence of flexural cracks.

The authors tested two beams consisting of one normal-strength concrete beam reinforced by steel bars and one UHPC beam reinforced by CFRP bars. The conventional (or normal-strength) beam served as a control specimen for comparison purposes. Both beams had a rectangular section of 203 mm (width) × 254 mm (depth) and were 4,270 mm long. The clear span of the beams between faces of bearings was 3,500 mm. A vertical force was applied at the beam midspan using a servo-controlled hydraulic actuator with a capacity of 978.6 kN.

2.2.2 Conventional Beam

As illustrated in Figure 5a, Grade 414 steel bars were provided consisting of two #22 bars at the bottom, two #13 bars at the top, and #10 stirrups spaced at 305 mm throughout the beam length. The compressive strength of concrete was 23.8 MPa at the time of testing. Figure 5b shows the beam prior to the test.

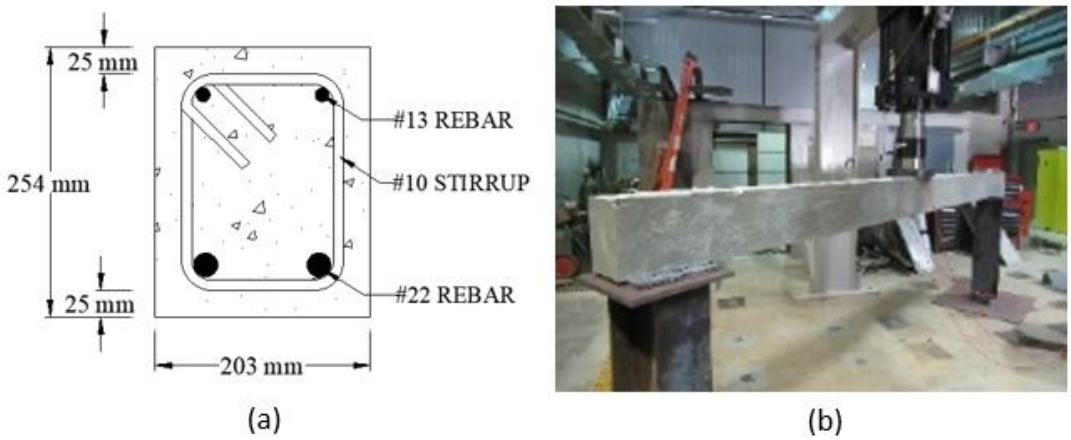

Figure 5 Conventional beam. (a) beam section and reinforcement detail. (b) beam prior to testing.

2.2.3 UHPC Beam Using CFRP Bars

The UHPC beam included two #10 Aslan CFRP bars at the bottom and two Grade 414 #13 steel bars at the top (Figure 6a). The size of the CFRP bars was identified to provide a comparable tension capacity to the #22 steel rebar in the conventional beam. Because the top reinforcement was not expected to contribute to the flexural strength substantially, steel bars were provided to allow for saving of material cost and ease of reinforcement placement. #10 steel stirrups were placed at half

of the span only with a spacing of 305 mm to study the effect of shear reinforcement on shear strengths between two beam ends. The compressive strength of UHPC was 130.9 MPa at the time of testing. Figure 6b shows the reinforcement placement in timber forms. Figure 7a presents the beam right after form removal. Figures 7b shows the beam prior to the test; the beam was painted to easily capture any cracks during the test.

Figure 6 UHPC beam reinforcement detail. (a) beam section. (b) reinforcement placement.

Figure 7 UHPC beam after concrete pour. (a) beam after form removal. (b) beam erected on supports.

3. Results and Discussions

3.1 Pullout Test Results

The bond stress versus slip relationship of the interface was developed to show the bond resistance corresponding to any given slip. Bond was quantified by the average bond strength (a stress unit), corresponding to the average shear strength achieved along the interface between the reinforcement and concrete matrix. The confinement effect in the loading direction was minimized by avoiding using a bearing plate at the prism face, because both reinforcement and its surrounding concrete were subject to tension in actual beams [32]. The applied load was monitored by a load cell and the slip data was recorded using a linear variable differential transducer (LVDT). The bond stress, σ, was determined using the following equation: $\sigma = P/(P_{ps}L)$, where P = applied load, L = embedment length, and P_{ps} = bar perimeter.

Plots of the bond stress versus slip for both conventional concrete (CC) and UHPC blocks were illustrated in Figure 8. In the plot for the UHPC specimen, the beginning of the diagram shows that the free-end slip occurred when the threshold shear stress reached approximately 5 MPa; chemical bond was the primary resisting mechanism in this stage. When the pullout load kept increasing, the slip started to grow and the friction bond mechanism became dominant. The pullout tests showed a first peak pullout load of about 40.6 kN corresponding to a slip of 0.5 mm, indicating exceptional bond behavior. These findings were comparable to the test results reported by Ahmad et al. [33], who further suggested a development length of approximately 40 times bar diameter for sand-coated CFRP bars. Also shown in Figure 8 was a plot for the conventional concrete specimen for comparison purposes. The free-end slip occurred when the threshold shear stress reached approximately 3 MPa, substantially lower than the UHPC specimen. Further, the conventional concrete failed abruptly when a maximum load of 27.7 kN was reached, while the UHPC specimen exhibited gradually increased slippage after the peak load, which attributed to the bridging effect of the steel fibers. Figure 9a shows the failure pattern in one specimen made of a UHPC block and a CFRP bar. Figures 9b and 9c show the plan and side views of the failure patterns in the conventional concrete block, respectively.

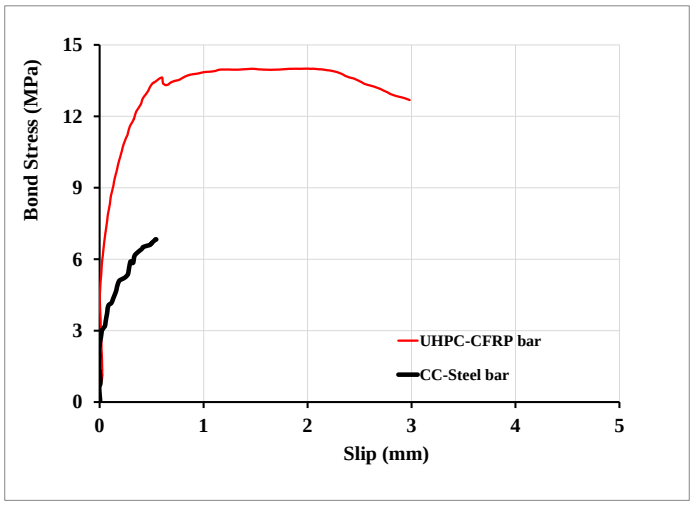

Figure 8 Stress versus slip diagrams.

Figure 9 Pullout tests. (a) failure pattern of a UHPC specimen with a CFRP. (b) failure pattern of a conventional concrete specimen (plan view). (c) failure pattern of a conventional concrete specimen (side view).

3.2 Test Results of the Large-scale Beams

The conventional beam failed when the load reached 90.3 kN after the tension reinforcement yielded and concrete at midspan crushed (Figures 10a and 10b). The UHPC beam started to crack near its midspan when the applied force reached 34.7 kN, which corresponded to a resulting tensile stress of approximately 13.8 MPa at the beam bottom (Figure 11a). The UHPC beam failed under an applied load of 101.9 kN when the CFRP bars reached its tensile strength (Figure 11b). The shear strength did not control the test over the flexural strength and neither beam ends exhibited any sign of shear failure even though half span did not include stirrups. As shown in Figure 12, the UHPC beam exhibited a higher loading capacity than the conventional beam, although only 2-#10 CFRP bars were used as compared to 2-#22 steel bars in the conventional beam. Prior to the flexural failure, the crack locations in the UHPC beam extended to a larger portion of the beam as compared to the conventional beam. Also, no concrete crushing occurred in the UHPC beam. As expected, the UHPC beam did not exhibit ductility as observed in the conventional beam because of the nonductile behavior of the CFRP bars. However, there was still sufficient warning of impending failure in a form of extensive cracking and substantial deflection because of the introduction of UHPC.

Figure 10 Conventional beam test. (a) beam during testing. (b) beam failure.

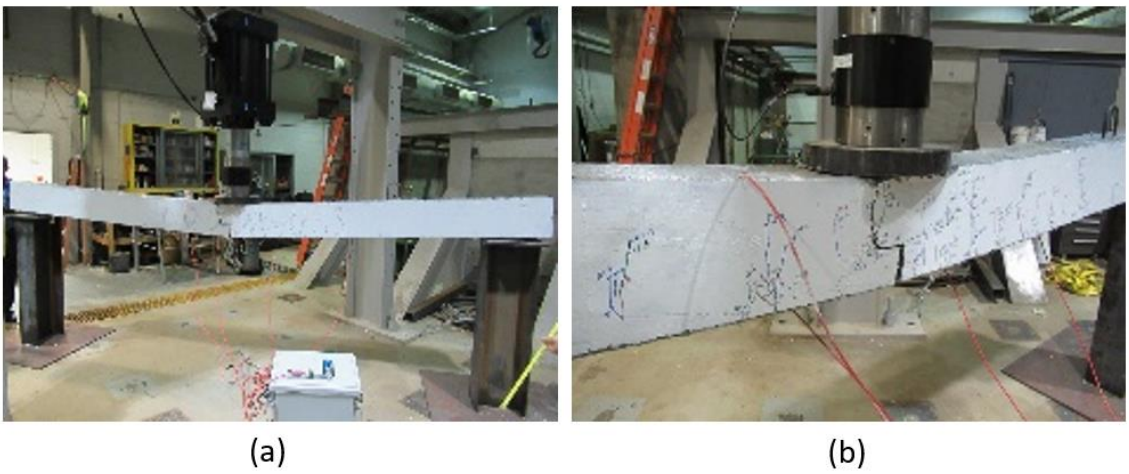

Figure 11 UHPC beam test. (a) beam during testing. (b) beam failure.

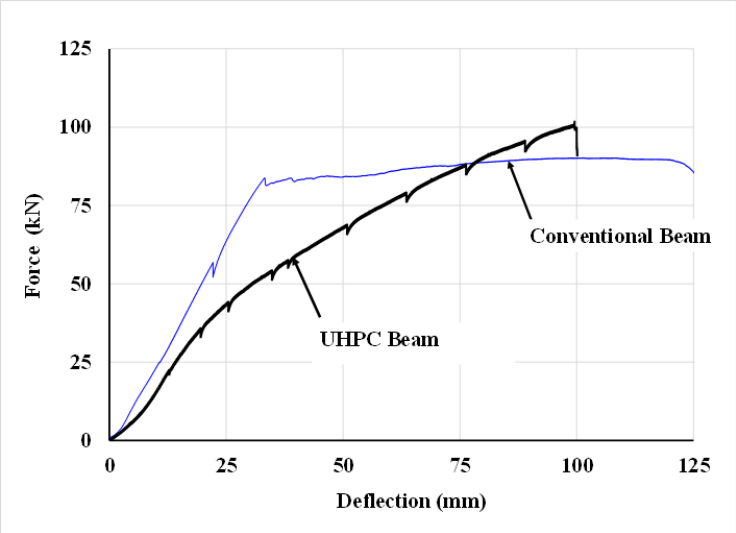

Figure 12 Force-deflection diagrams.

3.3 Analytical Study of the UHPC Beam Using CFRP Bars

The simply supported UHPC beam in Figures 6 and 7 was analyzed accounting for the CFRP and steel bars at the section bottom and top, respectively. Its flexural strength was determined following strain compatibility and force equilibrium [34]. Eq. 1 shows the strain compatibility approach accounting for both layers of steel and CFRP bars, and Eq. 2 provides the force equilibrium in the section. The stresses of steel and CFRP bars are given in Eqs. 3 and 4 following the elastic-plastic and elastic relationships, respectively. Variables in the equations are defined in the notations section.

$$\varepsilon_{si} = \varepsilon_c \left(\frac{d_i}{c} - 1 \right) \quad \text{(Eq. 1)}$$

$$\sum f_{si} A_{si} + \sum f_{cj} A_{cj} = 0 \quad \text{(Eq. 2)}$$

$$f_{s1} = E_{s1} \varepsilon_{s1} \leq f_y \quad \text{(Eq. 3)}$$

$$f_{s2} = E_{s2} \varepsilon_{s2} \quad \text{(Eq. 4)}$$

Two methods were taken to determine the flexural strength: Graybeal's and ACI 544's methods [35-37]. Figure 13 illustrates a cross section of the beam, strain diagram, and stress and force diagrams using both methods. The analyses adopted Graybeal's simplified UHPC stress-strain diagram for a commercial product (Figure 14), which has a compressive strength up to 165.4 MPa and a tensile strength of 10.3 MPa [35]. The concrete strain in Eq. 1 is related to modulus of elasticity, which is shown in Eq. 5 [35].

$$E_C = 3834\sqrt{f_c'} \quad \text{(Eq. 5)}$$

where f_c' is the UHPC compressive strength and its unit is in MPa.

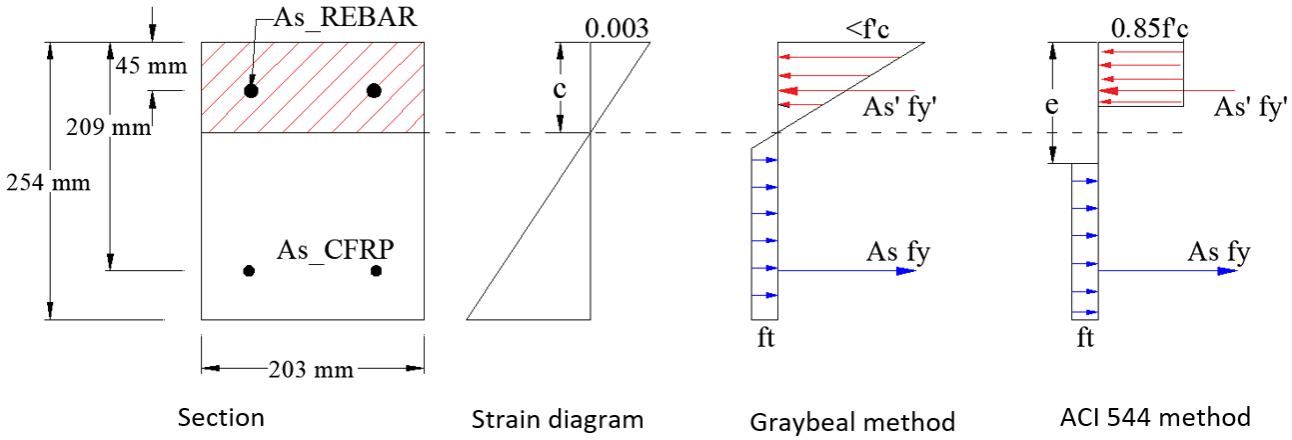

Figure 13 Flexural strength analysis per Graybeal and ACI 544 methods.

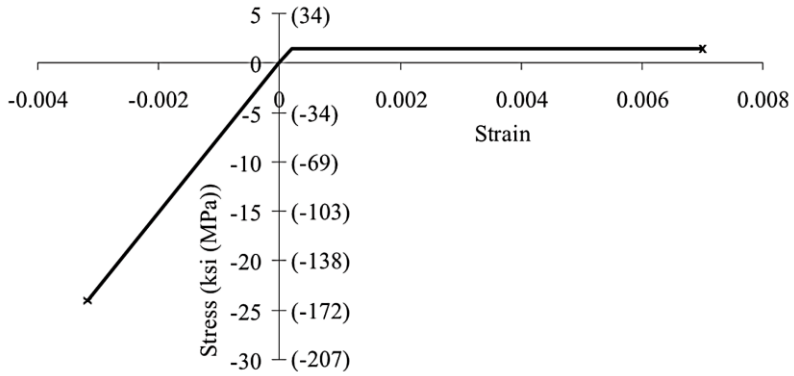

Figure 14 Simplified uniaxial stress-strain diagram for UHPC [35].

The calculated flexural strengths using Graybeal and ACI 544 methods were 68.5 kN-m and 72.9 kN-m, respectively, which were comparable. The calculated flexural strengths corresponded to a concentrated force of 78.3 kN and 83.3 kN at midspan, which were 23% and 18% lower than the actual loading capacity (101.9 kN) based on the laboratory test. It indicated that the assumed material properties and analysis methods were reasonably conservative.

To further evaluate the flexural strength analyses using Graybeal and ACI 544 methods, plots on the nominal flexural strengths versus steel ratios were provided in Figure 15 for a singly reinforced UHPC beam using CFRP bars. It was assumed that the UHPC beam was 203 mm wide by 254 mm deep. Reinforcement in the UHPC beam was the same as what was shown in Figure 6 except that no top reinforcement was included for simplicity. The steel ratios ranged from approximately 0.5% to 2.5%. Three compressive strengths of UHPC were accounted for: 144.8, 131.0, and 117.2 MPa. The dashed and solid lines in Figure 15 represent the strengths following the ACI 544 and Graybeal methods, respectively. It was found that both methods generated comparable results (up to 7% difference), while the ACI 544 method mostly resulted in slightly higher flexural strengths than the Graybeal method.

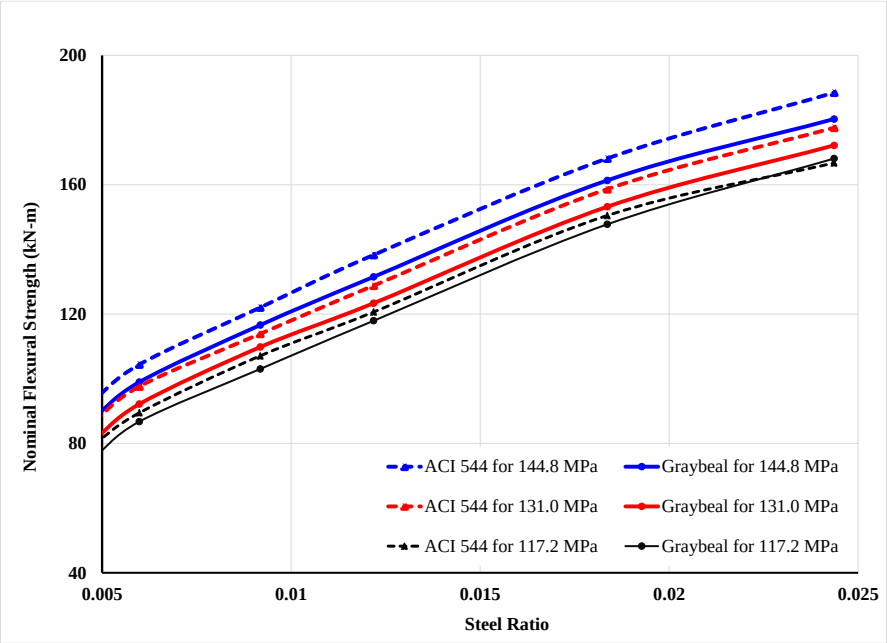

Figure 15 UHPC beam's nominal flexural strengths using ACI 544 and Graybeal methods.

4. Conclusions

This paper presents experimental and analytical studies of a UHPC beam reinforced by CFRP bars. Bond characteristics between the UHPC and CFRP bars were evaluated through pullout tests. Laboratory tests were conducted for large-scale UHPC and conventional beams to study their flexural behavior. This paper also addressed the flexural strength analysis of the UHPC beam accounting for strain compatibility and force equilibrium. The following conclusions were made:

1) In comparison with the conventional specimens made of normal strength concrete and steel rebar, pullout tests of the UHPC specimens showed that exceptional bond performance was achieved between the CFRP bar and UHPC prism.
2) Laboratory testing of both UHPC and conventional beams demonstrated that the UHPC beam did not exhibit as much ductility as observed in the conventional beam because of the nonductile behavior of the CFRP bars. However, there was still sufficient warning of impending failure in a form of extensive cracking and substantial deflection attributable to the bridging effect of the steel fibers in UHPC.
3) The flexural strength analyses using both Graybeal and ACI 544 methods accounted for strain compatibility and force equilibrium, which resulted in comparable flexural strengths. The predicted loading capacities of the UHPC beam using these methods were 18 to 23% lower than the test result, indicating that both methods were conservatively acceptable for design purposes.

Notations

ε_{si} = Strain of steel
ε_c = Strain of concrete
d_i = Distance from extreme compressive fiber to the center of steel bar
c = Distance from extreme compressive fiber to the neutral axis

$\Sigma f_{si} A_{si}$ = Total tension force
$\Sigma f_{cj} A_{cj}$ = Total compression force
f_{s1} = Tensile stress of steel at elastic range
E_{s1} = Modulus of elasticity of steel
ε_{s1} = Strain of steel at elastic range
f_y = Tensile strength of steel
f_{s2} = Tensile stress of steel at plastic range
ε_{s2} = Strain of steel at plastic range
E_C = Modulus of elasticity of concrete
f_c' = Compressive strength of concrete
f_t = Tensile strength of concrete

Acknowledgments

The authors would like to thank Mr. Chris Morgan and Dr. Omar Abdulkareem for assisting in the lab testing.

Author Contributions

C. Shawn Sun: original draft preparation, supervision, analysis, experiment. Nahid Farzana: analysis, experiment. Dinesha Kuruppuarachchi, Mohammadamin Azimi, and Huayuan Zhong: experiment.

Funding

Not applicable.

Competing Interests

The authors have declared that no competing interests exist.

References

1. Koch GH, Brongers MP, Thompson NG, Virmani YP, Payer JH. Corrosion cost and preventive strategies in the United States. Washington, DC: Federal Highway Administration, Office of Infrastructure Research and Development; 2002; No. FHWA-RD-01-156.
2. Moser R, Holland RB, Kahn L, Singh P, Kurtis K. Durability of precast prestressed concrete piles in marine environment: Reinforcement corrosion and mitigation–Part 1. Atlanta, GA: Office of Materials and Research, Georgia Department of Transportation; 2011; ID# 20616.
3. Bentur A, Berke N, Diamond S. Steel corrosion in concrete: Fundamentals and civil engineering practice. London: CRC press; 2014.
4. Griggs RD. Structural concrete in the Georgia coastal environment. Atlanta, GA: Georgia GDOT; 1987.
5. Federal Highway Administration. Status of the nation's highways, bridges, and transit: Conditions and performance. Washington, DC: Federal Highway Administration; 2006.
6. Mehta PK. Concrete in the marine environment. Boca Raton: CRC Press; 1991.

7. Gries MB, Michols KA, Lawler JS, Whitmore DW, Miltenberger M. Evaluation and repair of natural draft cooling towers. Proceedings of the CORROSION 2018; 2018 April 15; Phoenix, Arizona, USA. Richardson, TX: OnePetro.
8. Joshi K. Investigation of carbon fiber composite cables (CFCC) in prestressed concrete piles. Tallahassee, FL: The Florida State University; 2013.
9. Fam AZ, Rizkalla SH, Tadros G. Behavior of CFRP for prestressing and shear reinforcements of concrete highway bridges. Struct J. 1997; 94: 77-86.
10. Poudel P, Belarbi A, Dawood M, Gencturk B, Acun B. Prestressing bridge girders with carbon fiber–reinforced polymer: State of knowledge and research needs. Adv Struct Eng. 2018; 21: 598-612.
11. American Concrete Institute Committee 440. Guide for the design and construction of structural concrete reinforced with FRP bars. Farmington Hills, MI: American Concrete Institute Committee 440; 2015; ACI 440.1R-15.
12. Belarbi A. Guide specification for the design of concrete bridge beams prestressed with CFRP systems. Washington, DC: TRB; 2018; Report No. CFRP-1-UL.
13. AASHTO. AASHTO LRFD bridge design specifications. 9th ed. Washington, DC: AASHTO; 2020.
14. Russell HG, Graybeal BA, Russell HG. Ultra-high performance concrete: A state-of-the-art report for the bridge community. Washington, DC: Federal Highway Administration, Office of Infrastructure Research and Development; 2013; No. FHWA-HRT-13-060.
15. Graybeal BA. Material property characterization of ultra-high performance concrete. Washington, DC: Federal Highway Administration, Office of Infrastructure Research and Development; 2006; No. FHWA-HRT-06-103.
16. Chao SH, Naaman AE, Parra-Montesinos GJ. Bond behavior of reinforcing bars in tensile strain-hardening fiber-reinforced cement composites. ACI Struct J. 2009; 106: 897.
17. Achillides Z, Pilakoutas K. Bond behavior of fiber reinforced polymer bars under direct pullout conditions. J Compos Constr. 2004; 8: 173-181.
18. Guadagnini M, Pilakoutas K, Waldron P, Achillides Z. Tests for the evaluation of bond properties of FRP bars in concrete. In: 2nd International Conference on FRP Composites in Civil Engineering. London: Taylor & Francis; 2004. pp. 343-350.
19. Borosnyói A. Influence of service temperature and strain rate on the bond performance of CFRP reinforcement in concrete. Compos Struct. 2015; 127: 18-27.
20. Grace NF, Navarre FC, Nacey RB, Bonus W, Collavino L. Design-construction of bridge street bridge-first CFRP bridge in the United States. PCI J. 2002; 47: 20-35.
21. Shim J. Prediction of early-age cracking of UHPC materials and structures: A thremo-chemo-mechanics approach. Cambridge, MA: Massachusetts Institute of Technology; 2005.
22. Yoo DY, Park JJ, Kim SW, Yoon YS. Early age setting, shrinkage and tensile characteristics of ultra high performance fiber reinforced concrete. Constr Build Mater. 2013; 41: 427-438.
23. Zhang Y. Whole life cycle cost for Chicago type bascule bridges. Cost Eng. 2008; 50: 28-32.
24. Huang L, Su L, Xie J, Lu Z, Li P, Hu R, et al. Dynamic splitting behaviour of ultra-high-performance concrete confined with carbon-fibre-reinforced polymer. Compos Struct. 2022; 284: 115155.
25. Kromoser B, Preinstorfer P, Kollegger J. Building lightweight structures with carbon-fiber-reinforced polymer-reinforced ultra-high-performance concrete: Research approach, construction materials, and conceptual design of three building components. Struct Concr. 2019; 20: 730-744.

26. Khalil N, Assaad JJ. Bond properties between smooth carbon fibre-reinforced polymer bars and ultra-high performance concrete modified with polymeric latexes and fibres. Eur J Environ Civ Eng. 2022; 26: 6211-6228.
27. Si-Larbi A, Ferrier E, Hamelin P. Flexural behaviour of Ultra High Performance Concrete reinforced with mixed short fibers and CFRP rebars. Proceedings of the International Symposium on Ultra High Performance Concrete; 2004 September 13-15; Kassel, Germany. Kassel: Kassel University Press. pp. 661-672.
28. Aronoff J, Katz A, Frostig Y. The behavior of very high strength concrete structures with CFRP reinforcing bars. Proceedings of the International Symposium on Ultra High Performance Concrete; 2004 September 13-15; Kassel, Germany. Kassel: Kassel University Press. pp. 547-558.
29. Alkhrdaji T, Fyfe ER, Karbhari VM, Schupack M, Bakis CE, Ganjehlou A, et al. Guide Test methods for fiber-reinforced polymers (FRPs) for reinforcing or strengthening concrete structures. Farmington Hills, MI: American Concrete Institute; 2004; ACI 440.3R-04.
30. American Society for Testing Materials. Standard practice for fabricating and testing specimens of ultra-high performance concrete. West Conshohocken, PA: American Society for Testing Materials; 2017; ASTM C1856/C1856M-17.
31. Ashtiani MS, Dhakal RP, Scott AN, Bull DK. Cyclic beam bending test for assessment of bond–slip behaviour. Eng Struct. 2013; 56: 1684-1697.
32. Chao SH. Bond characterization of reinforcing bars and prestressing strands in high performance fiber reinforced cementitious composites under monotonic and cyclic loading. Ann Arbor: University of Michigan; 2005.
33. Ahmad FS, Foret G, Le Roy R. Bond between carbon fibre-reinforced polymer (CFRP) bars and ultra high performance fibre reinforced concrete (UHPFRC): Experimental study. Constr Build Mater. 2011; 25: 479-485.
34. PCI Bridge Design Manual Steering Committee. Precast prestressed concrete bridge design manual. Chicago, IL: PCI; 2014; MNL-133-11.
35. Graybeal BA. Flexural behavior of an ultrahigh-performance concrete I-girder. J Bridge Eng. 2008; 13: 602-610.
36. Shafieifar M, Farzad M, Azizinamini A. A comparison of existing analytical methods to predict the flexural capacity of Ultra High Performance Concrete (UHPC) beams. Constr Build Mater. 2018; 172: 10-18.
37. American Concrete Institute Committee 544. Design considerations for steel fiber reinforced concrete. Farmington Hills, MI: American Concrete Institute Committee 544; 1988; ACI 544.4R-88.